Pharm Res (2020) 37: 144
https://doi.org/10.1007/s11095-020-02836-6

RESEARCH PAPER

Dicationic Amino Substituted Gemini Surfactants and their Nanoplexes: Improved Synthesis and Characterization of Transfection Efficiency and Corneal Penetration *In Vitro*

Lokesh Narsineni [1] • Marianna Foldvari [1,2]

Received: 29 February 2020 / Accepted: 29 April 2020 / Published online: 14 July 2020

ABSTRACT

Purpose To formulate and characterize nanoparticles from m-7NH-m gemini surfactants, synthesized by a new improved method, for non-invasive gene delivery including optimization of composition for transfection efficiency and corneal penetration.

Methods A one-pot, solvent-free, DMAP-free method was developed for the synthesis of m-7NH-m (m = 12–18) gemini surfactant series. Lipoplexes (LPXs) and nanoplexes (NPXs) of gemini surfactant-plasmid DNA were formulated with and without DOPE helper lipid, respectively, at various charge ratios and characterized by dynamic light scattering and zeta potential measurements. Transfection efficiency, cellular toxicity, effect of DOPE and gene expression kinetic studies were carried out in A7 astrocytes by flow cytometry and confocal microscopy. Corneal penetration studies of 18-7NH-18 NPXs were carried out using 3D EpiCorneal® tissue model.

Results The new synthesis method provides a two-fold improved yield and the production of a pure species of m-7NH-m without DMAP and trimeric m-7N(m)-m surfactants as impurities. Structure and purity was confirmed by ESI-MS, ^{1}H NMR spectroscopy and surface tension measurements. Particle size of 199.80 ± 1.83 nm ± S.D. and a zeta potential value of +30.18 ± 1.17 mV ± S.D. was obtained for 18-7NH-18 5:1 ratio NPXs showed optimum transfection efficiency (10.97 ± 0.11%) and low toxicity (92.97 ± 0.57% viability) at the 48-h peak expression. Inclusion of DOPE at 1: 0.5 and 1:1 ratios to gemini surfactant reduced transfection efficiency and increased toxicity. Treatment of EpiCorneal® tissue model showed deep penetration of up to 100 μm with 18-7NH-18 NPXs.

Conclusion Overall, 18-7NH-18 NPXs are potential gene delivery systems for ophthalmic gene delivery and for further *in vivo* studies.

KEY WORDS confocal microscopy · cornea · flow cytometry · gemini surfactant · gene expression · neurotrophic factors · non-viral gene delivery

ABBREVIATIONS

CMC	Critical micelle concentration
CLSM	Confocal laser scanning microscope
DOPE	1,2-Dioleoyl-sn-glycero-3-phosphoethanolamine
DMAP	4-(Dimethylamino)pyridine
ESI-MS	Electro-spray ionization mass spectrometry
GP	gemini:plasmid
GPL	gemini:plasmid:lipid
GFP	Green fluorescent protein
^{1}H NMR	Proton- nuclear magnetic resonance spectroscopy
LPX	Lipoplex
NPX	Nanoplex
TE	Transfection efficiency
TFA	Trifluoroacetic acid
TIS	Triisopropylsilane
DMEM	Dulbecco's modified eagle's medium
FBS	Fetal bovine serum

Guest Editor: Sheng Qi

✉ Marianna Foldvari
foldvari@uwaterloo.ca

[1] School of Pharmacy, University of Waterloo, 200 University Avenue West, Waterloo, Ontario N2L 3G1, Canada

[2] School of Pharmacy, Center for Bioengineering and Biotechnology, Waterloo Institute of Nanotechnology, University of Waterloo, 200 University Avenue West, Waterloo, Ontario N2L 3G1, Canada

INTRODUCTION

Gemini surfactants are dicationic amphiphilic biomaterials that have shown potential for use in gene therapy. Since their first discovery in the early 1970s (1,2) and the recognition of their unique properties in the early 1990s (3,4), gemini surfactants have been investigated as potential nanomaterials for various diverse applications. One of these applications is as cationic vectors for gene delivery (5,6). A unique feature that allows them to be a strong gene delivery vectors is the cationic charges in the polar head group of gemini surfactant molecule. The positively charged quaternary nitrogen head groups bind to and compact the DNA into smaller particle size due to electrostatic interactions, and promote enhanced uptake into cells (7–9).

Gemini surfactant chemistry is quite versatile, and several groups, including ours, created compound libraries with varying alkyl tail lengths and spacer groups (10–13). For example, modification of the simple polymethylene spacer of m-s-m first generation gemini surfactants with an amino group, produced m-7NH-m second generation gemini surfactants with pH-sensitive functionality (11–13). Additionally, this amine substituted gemini compound library with varying carbon chain length serves as the parent compounds for the third generation peptide-conjugated gemini surfactants (14–17) to enhance gene delivery.

Early synthesis of gemini molecules was carried out with ionic head groups and a rigid spacer by reacting α,α'-di-bromo-*p*-xylene with a dianionic long-chain alkyl phosphate and another series by phosphorylating with $POCl_3$. The resulting compounds were purified by recrystallization as sodium salts (18,19). The synthesis of m-s-m surfactants that is now routinely followed is a one-step process where the appropriate α,ω-dibromoalkane (according to spacer length required) is reacted with approximately 2 M equivalents of the appropriate N,N-dimethylalkylamine (20,21).

Our group reported the synthesis of the amine-substituted gemini surfactants by reacting 3,3′-iminobis(N,N-dimethylpropylamine) with approximately 2 M equivalents of the appropriate 1-bromoalkane in acetonitrile (Fig. 1a) (12). This method was later modified to include a Boc_2O protection, deprotection and multiple recrystallization steps to purify the final product (Fig. 1b). In this method the Boc_2O group helps to protect the amine group in the 3,3´-iminobis(N,N-dimethylpropyl-amine), before proceeding with the quaternization, which is important to prevent the nucleophilic attack on the NH group by 1-bromoalkane. In the reaction 4-(dimethylamino) pyridine (DMAP) is used as catalyst to speed up the reaction during the Boc_2O protection (12,22). This method involves multiple steps and uses large amounts of chemicals and solvents to synthesize the final products. In addition, during the purification steps, the recrystallizations result in yields that are often lower than 40% DMAP and other by-products may remain as a contaminant after the final recrystallization. We have also identified that these synthetic schemes, in addition to the dimeric (m-7NH-m) also produce a trimeric (m-7N(m)-m) gemini compound with 3 alkyl tails. Multiple recrystallizations and purification, using various methods failed to separate these two species in the final product, as verified through ^{1}H NMR and mass spectrometry.

To address these issues, a solvent-free, DMAP-free synthesis of m-7NH-m gemini surfactant was developed by adapting a one-pot synthesis technique (23) to yield pure m-7NH-m gemini surfactant. In the one-pot reaction scheme the protection and nucleophilic bond formation steps are incorporated into a single reaction without multiple recrystallization. This approach saves time, chemicals, and more importantly, provide higher yields of the final product. Also, a solvent-free technique was adapted for Boc_2O protection of the amine group in the spacer (24). Then we have formulated and characterized nanoparticles from m-7NH-m gemini surfactants, synthesized by the new improved synthetic method, for gene delivery including optimization of composition for transfection efficiency (TE) to A7 astrocytes as potential target cells and corneal penetration. We have also compared m-7NH-m gemini surfactants made by the previous and the new synthesis method, with specific interest in evaluating the effect of the trimeric (m-7N(m)-m) gemini compound that can be present as a by-product in previous batches.

MATERIALS AND METHODS

Synthesis of m-7NH-m Dimeric Gemini Surfactants

Two methods were used for the synthesis of m-7NH-m (m = 12, 16 and 18) gemini surfactants. *Method 1* followed a previously reported method (8,12,18–20) and *Method 2* is the new of one-pot, DMAP- free technique. The general scheme and the two synthesis methods of m-7NH-m (m = 12, 16 and 18) gemini surfactants are illustrated in Fig. 1 (a, b and c).

All reactions were carried out under nitrogen environment using Radley's Carousel 6 Plus reaction station™ (Saffron Walden, Essex, UK). Reaction materials were purchased from Sigma-Aldrich (Oakville, ON, Canada): 3,3′-iminobis(N,N-dimethylpropylamine), (MW: 187.33 g/mol, 97%), di-t-butyl dicarbonate (Boc_2O) (MW: 218.25 g/mol, >99%), acetonitrile anhydrous (MeCN) (99.8%), 1-bromododecane (MW:249.24 g/mol, 97%), 1-bromohexadecane (MW:305.33 g/mol, 97%), 1-bromooctadecane (MW:333.38 g/mol, 97%), trifluoroacetic acid (TFA) (MW:114.02 g/mol, 99%), triisopropylsilane (TIS) (MW:158.36 g/mol, 98%). For analysis ^{1}H NMR Spectroscopy (Bruker Avance 300 and 500, Bruker, MA, USA) and electron spray ionization mass spectrometry (ESI-MS) (Thermo Q-Exactive with Orbitrap, Thermo-Fisher Scientific, CA, USA) was used.

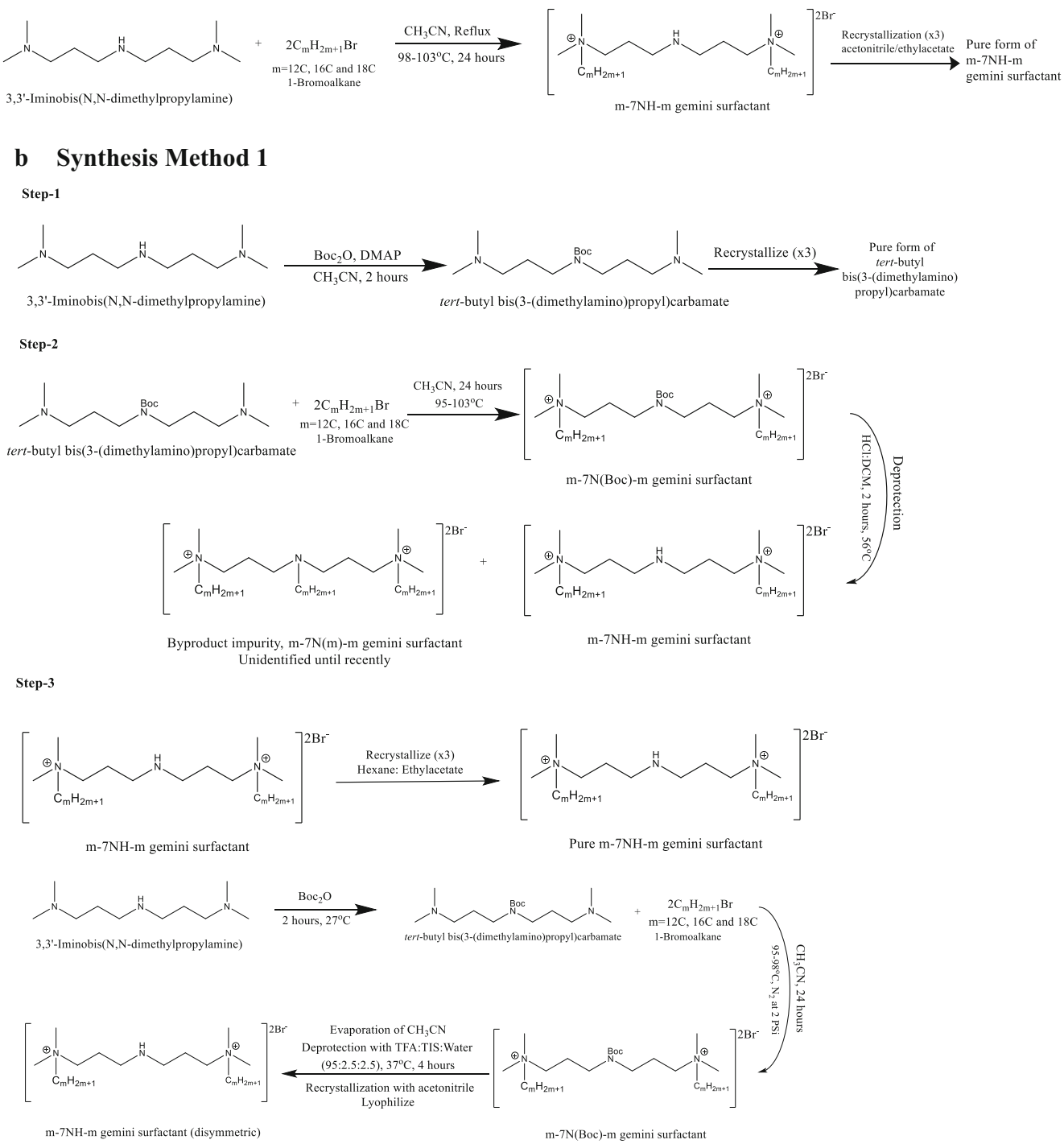

Fig. 1 Synthesis schemes of dimeric gemini surfactants with a spacer amine functional group and its as building blocks for nanoparticles, (**a**) General scheme for synthesis of m-7NH-m dimeric gemini surfactants, (**b**) Synthesis method 1: synthesis of m-7NH-m dimeric gemini surfactants, (**c**) Synthesis method 2: improved synthesis of m-7NH-m dimeric gemini surfactants using solvent-free, DMAP-free, Boc_2O protection with a one-pot technique, (**d**) Surface tension *vs* log concentration plot for the 18-7NH-18 gemini surfactant. CMC value is the point where surface tension dissects the concentration plot. All surface tension measurements were obtained by applying Harkin-Jordan's correction.

Synthesis for m-7NH-m surfactants using the previously reported and routinely used method (Fig. 1b) was carried out as follows: one equivalent of 3,3′-iminobis(N,N-dimethylpropylamine) with 2.2 equivalents of 1-Bromododecane were refluxed in acetonitrile for 24 h and the product was purified by recrystallization using acetonitrile/

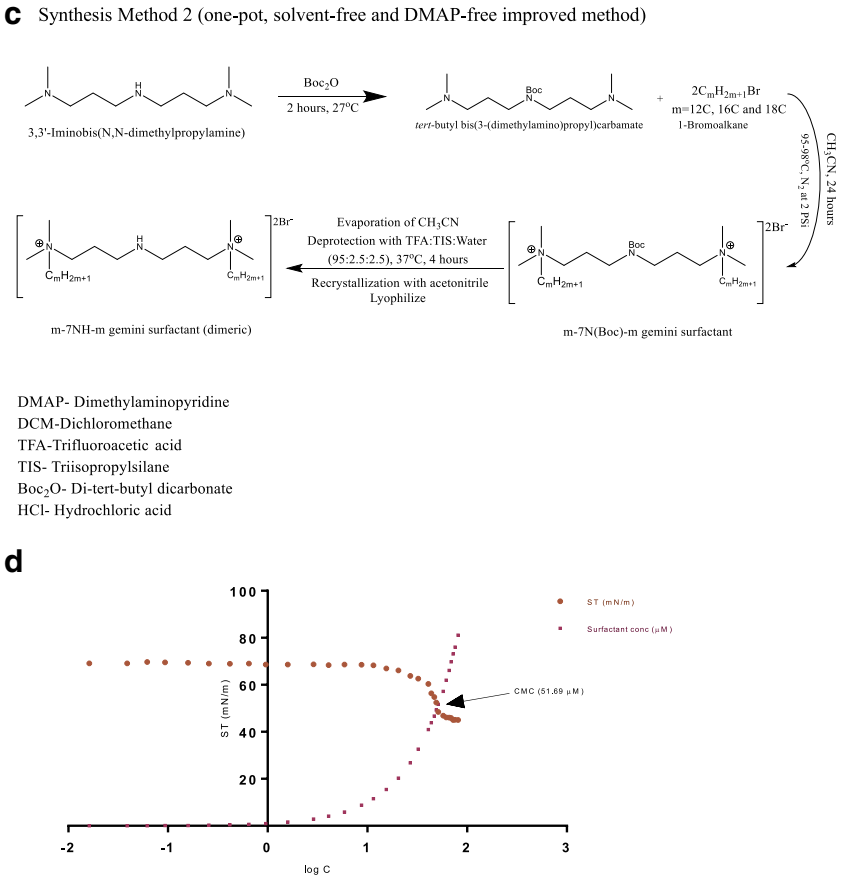

Fig. 1 (Continued)

ethyl acetate (12). While in the modified group a Boc_2O protection with DMAP as catalyst and deprotection using DCM:HCl was used. With the improved method shown in Fig. 1c, the gemini surfactant synthesis using the one-pot, solvent-free Boc_2O protection and DMAP- free technique with amino substitution spacers was carried out in a Radleys reaction flask by Boc_2O protection of 1 equivalent (0.01 M) of 3,3′-iminobis(N,N-dimethylpropylamine) using a 1.2 equivalent (0.012 M) of Boc_2O reagent directly without use of any other solvent (24). The reaction mixture was stirred at 27°C for 4 h. Once the protection reaction was complete, 50 mL/3 g theoretical yield of acetonitrile was added to the reaction vessel, followed by 2.1 equivalents of either 1-bromododecane (12-7NH-12) or 1-bromohexadecane (16-7NH-16) or 1-bromooctadecane (18-7NH-18) and the reaction was run under nitrogen atmosphere at 2 Psi, and 95°C for 24 h. Completion of the reaction was monitored using thin layer chromatography (TLC) on silica gel plates (TLC silica gel 60 F_{254}, Merck, MA, USA) and visual spots were developed using iodine vapors. After 24 h, the reaction flask was cooled down and the precipitate was filtered and recrystallized using acetonitrile three times. Deprotection was carried out using TFA cleavage cocktail TFA/TIS/Water (95:2.5:2.5) and the excess TFA was evaporated by flushing with nitrogen and traces of TFA was evaporated in vacuo by using a Heidolph Hei-VAP Core rotary evaporator (Heidolph Instruments GmBH & CO. KG, Schwabach, Germany). Precipitate was extracted by adding water into the flask to dissolve the pure surfactant, lyophilized using a Labconco Freezone 1 freeze dryer (Labconco, MO, USA) to obtain pure m-7NH-m gemini surfactant. Purity and identification of the surfactants was assessed using mass spectrometry, ^{1}H NMR spectroscopy (Avance 500 MHz) using $CDCl_3$ as a solvent and surface tension measurement was carried out using a du Nuoy ring tensiometer (Lauda TE3 automated tensiometer, Lauda, Germany).

Analysis of Gemini Derivatives

Mass spectrometry analysis was by electron spray ionization mass spectrometry (ESI-MS) (Thermo Q-Exactive with Orbitrap, Thermo-Fisher Scientific, CA, USA). ^{1}H NMR Spectroscopy analysis was carried out on Bruker Avance 500 MHz instrument by dissolving the sample in the $CDCl_3$ solvent and the chemical shifts obtained were confirmed.

18-7NH-18 (new stock, **NS)** ESI-MS: Chemical formula- $C_{46}H_{99}N_3^{2+}$, molecular weight: 694.32 (without Br^- counter ions), 854.13 (with 2 Br^-), charge ratio: +2, expected peaks m/z: 346.89, found peaks m/z: 346.89, yield-70-73%.

18-7NH-18 (old stock, **OS**: both 18-7NH-18, 18-7 N(18)-18 gemini surfactants and DMAP. Molecular weight: 18-7NH-18: 694.32 (without Br^- counter ions), 854.13 (with 2 Br^-); molecular weight of 18-7 N(18)-18: 946.80 (without Br^-), 1106.61 (with $2Br^-$) counter ions. m/z identified in the OS: 346.89, 473.03 and 123.09 for 18-7NH-18, 18-7 N(18)-18 gemini surfactants, charge ratio: +2, and DMAP, respectively.

Formulation of Dimeric Gemini Nanoplexes and Lipoplexes

Nanoparticles of dimeric (synthesized by the two different methods Fig. 1 b and c) (m = 12, 16 and 18 C, alkyl tail) gemini surfactants were prepared with or without DOPE (Avanti Polar Lipids, Alabaster, AL, USA). Nanoplexes (NPXs) are composed of gemini surfactant and plasmid and lipoplexes (LPXs) are composed of gemini surfactant, plasmid and DOPE. The NPXs and LPXs were prepared at 2.5:1, 5:1, 7.5:1 and 10:1 (gemini surfactant: plasmid; G:P) charge (ρ±) ratios (ratio of positively charged nitrogens on the gemini surfactant to the negatively charged phosphate groups on the phosphate backbone of DNA) and 1:0.5 and 1:1 (gemini surfactant: DOPE; G:L) mass ratio, respectively. NPX formulations were made by mixing the required amount of plasmid solution with a calculated volume of gemini surfactant stock solution to obtain the required ρ±. The mixtures were left at room temperature for 15 min. LPX formulations were made by mixing the plasmid first with gemini surfactant to get required ρ ± ratio and incubation for 15 min followed by addition of DOPE helper lipid vesicles, prepared at 5 mM concentration in 9.25% (*w/v*) sucrose solution at pH 9, using an LV1 Microfluidizer (Microfluidics Corporation, Newton, MA, USA) at the required gemini: DOPE ratio and mixed by brief vortexing.

Characterization of Gemini Surfactants

CMC Determination

Surface tension measurements for 18-7NH-18 were carried out using the du Noüy ring tensiometry method on a Lauda TE3 model automated tensiometer (Lauda, Germany). The surface tension was measured after calibrating the tensiometer using standard weights. The vessel was filled with 40 mL of ultrapure water and the concentrated surfactant solution (130 μmol/L) was titrated into the ultrapure water and the surface tension was measured after every addition. The water bath was kept at 45°C ± 0.1°C during the surface tension measurements. Surface tension measurements were subjected to Harkin and Jordan's correction and the obtained values were used to determine the CMC value by plotting on a surface tension *vs* logarithmic concentration plot.

Particle Size and Zeta Potential Analysis

Particle size distribution and polydispersity index (PDI) of NPXs and LPXs was determined by dynamic light scattering (DLS) using Zetasizer Nano ZS (Malvern Instruments, Worcestershire, UK) sample Z-average size of each sample was reported as an average of three readings±S.D. Zeta potential measurement was carried out after dilution of formulations with ultrapure water at 1:25 (v/v) ratio and reported as mV ± S.D. (n = 6 readings).

Transfection Efficiency and Viability Studies by Flow Cytometry

Rat A7 astrocytes (received from Dr. Jeremy Sivak, University of Toronto) were cultured in DMEM/high glucose media (Hyclone, GE Healthcare Life Sciences, Logan, Utah, USA) supplemented with 10% FBS (Hyclone, GE Healthcare Life Sciences, Logan, UT, USA) and 1% Pen/Strep (Hyclone, GE Healthcare Life Sciences, Logan, Utah, USA) at 37°C in a 95% air/5% carbon dioxide. 15,000 cells/well were seeded in 96 well flat bottom tissue culture plates (Grenier Bio-one, Monroe, NC, USA). After 24 h at 80–90% confluency, complete media was removed from the plate and replaced with fresh serum-free basic media. Cells were treated with formulations containing 0.5 μg of pDNA treatment dose per well and incubated for 5 h at 37°C. Lipofectamine 3000 (Invitrogen, Thermo Fisher Scientific, Waltham, MA, USA) was used as a reference standard, and plasmid only and untreated tissues as controls. After the incubation cells were detached using Accutase™ and stained with MitoTracker Deep Red FM (500 nM) (Thermo Fisher Scientific), prepared as a 1000 nM stock in Accumax™ (cell dissociation solution) (Innovative Cell Technologies, San Diego, CA, USA) and incubated for 30 min. After incubation, TE (%) and viability (total live population %) were analyzed by Attune flow cytometer (Life Technologies, Carlsbad, CA, USA).

Kinetics of Gene Expression in A7 Astrocytes Treated with NPXs

To establish the gene expression kinetics for gemini NPXs, A7 astrocyte cells were plated in 96 well plates at 15,000 cells/well. At 80% confluency they were treated with gemini NPXs at 2.5, 5:1 and 7.5:1 (G:P) ρ ± ratios. Each plate was analyzed at 24, 48 and 72 h incubation for TE and viability using flow cytometry with Mitotracker™ Deep Red as viability stain and confocal microscopy with DRAQ5 as nuclear stain. The effect of gemini NPXs incubation time on TE and viability was assessed after the removal of NPXs at the 5h time point or after continuous exposure for the total incubation.

Statistical Analysis

All statistical analyses were carried out using GraphPad Prism (GraphPad Software, San Diego, CA, USA). Data are presented as mean ± S.D., ($n = 3$). Two-way ANOVA with Tukey multiple comparison tests were carried out to analyze the obtained data sets. A P value less than 0.05 was considered as significant and the level of significance is indicated in the figure legends.

In Vitro Corneal Penetration Studies Using 3D EpiCorneal™ Model

Corneal tissue penetration studies were carried out using EpiCorneal COR-100 3D human corneal tissue model (MatTek Corporation, Ashland, MA). Cy5 labelled gWIZ-GFP was used to track the movement and gene expression of NPXs in the corneal tissue after treatment. Cy5 labelling of gWIZ plasmid was performed using Label IT® reagent (Mirus Bio LLC., Madison, WI) according to manufacturer's protocol at 0.5:1 dye: pDNA ratio for 1 h at 37°C.

Each well received 2.5 µg of Cy5 labelled gWIZ-GFP/ 50 µL dose of 18-7NH-18 5:1 NPX formulations. Briefly, on the day of the experiment after the equilibration of the tissues, media was aspirated from each well and replaced with 1 mL fresh, prewarmed media and incubated for 1 h. Tissues in each well were dosed with NPXs. After dosing the tissues were returned to the CO_2 incubator tissues were isolated from the plate at 0.5 and 1 h, washed with phosphate buffer saline (PBS) three times to simulate removal of surface-bound NPXs by tear, and stained with Calcein AM (Invitrogen) as a live cell stain and Image IT® (Invitrogen),) as a dead cell stain and processed for imaging using confocal laser scanning microscope (CLSM).

RESULTS AND DISCUSSION

To develop a topical gene delivery system for ocular administration with the ultimate goal to reach the retina requires crossing tough barriers within the eye and demands the design of a delivery system that has a suitable combination of properties, such as sufficient residence time within the precorneal surface, permeability to the posterior segment of the eye, suitable TE, biocompatibility and pharmaceutical properties. We have formulated a novel nanoparticle system based on the 18-7NH-18 s-generation gemini surfactant and evaluated their transfection properties and interaction with the corneal surface. Compared to previously studied gemini derivatives, 12-7NH-12 and 16-7NH-16 (12,13), the 18C long alkyl tail may provide advantages for topical application, including higher TE (25).

We have developed an improved synthesis method for m-7NH-m gemini surfactants, which is simpler and uses a solvent-free and DMAP free approach for Boc_2O protection compared to previous methods (Fig. 1, b and c). The main improvements were the introduction of a one-pot solvent-free Boc_2O protection step and the exclusion of DMAP, a non-recyclable solvent and catalyst, and a potential contaminant in the final purified products. The analysis of structure, molecular weight assessments and purity was confirmed by ESI-MS, ^{1}H NMR spectroscopy and surface tension measurements. The purity level with the new method were improved from 55 to 60% to 95–98% and the yield improved from about 40% to 72–78% as calculated from the theoretical yield compared with the actual yield of the products.

In addition to the approximately two-fold better yield and 'green' solvent-free one-pot approach, the improved synthesis method presented here provides two additional crucial advantages. The use of DMAP provides a significant challenge with purification and can remain at various levels as an impurity in the final product even after multiple recrystallizations. This could be due to the strong interaction of the DMAP with the quaternary nitrogens. During the reaction another derivative (previously unidentified), a trimeric m-7N(m)-m can also form at different levels depending on the conditions used and its removal during purification may not be easily achieved. As shown in Fig. 1 a and b, the lack of suitable protection and deprotection steps on the spacer tertiary amine group, specifically the deprotection with DCM: HCl at 56°C at the end of the reaction, before recrystallization of the Boc-protected gemini surfactant could have led to cross-reaction between bromoalkanes and the tertiary amine group in the spacer (Fig. 1b). Using the solvent- and DMAP-free Boc_2O protection before quaternization and TFA deprotection at the end of synthesis after recrystallization of the Boc_2O protected final product produces pure m-7NH-m without DMAP and/or trimeric m-7N(m)-m surfactant as impurities, and the one-pot reaction scheme allows for increased yield with low product loss that typically occurs with multiple recrystallizations in a multi-step synthetic scheme.

The purity of the newly synthesized 18-7NH-18 was confirmed from the surface tension *vs* log concentration plot by carrying out regression analysis. The CMC value was determined to be 51.69 µM (Fig. 1d). This CMC value is different from the previously reported CMC value of 13 µM (13), which was expected due to improved purity obtained in this work. The increased hydrophobicity of the m-7N(m)-m gemini surfactant, if present as an impurity, would contribute to lower CMC values (26). In this regard, it is possible that in our previous paper the 18-7NH-18 compound may have contained this trimeric impurity (13).

Particle size of m-7NH-m gemini NPXs varied between 180 and 320 nm depending on the charge ratio and the presence of DOPE lipid in the formulation (Fig. 2b). Gemini

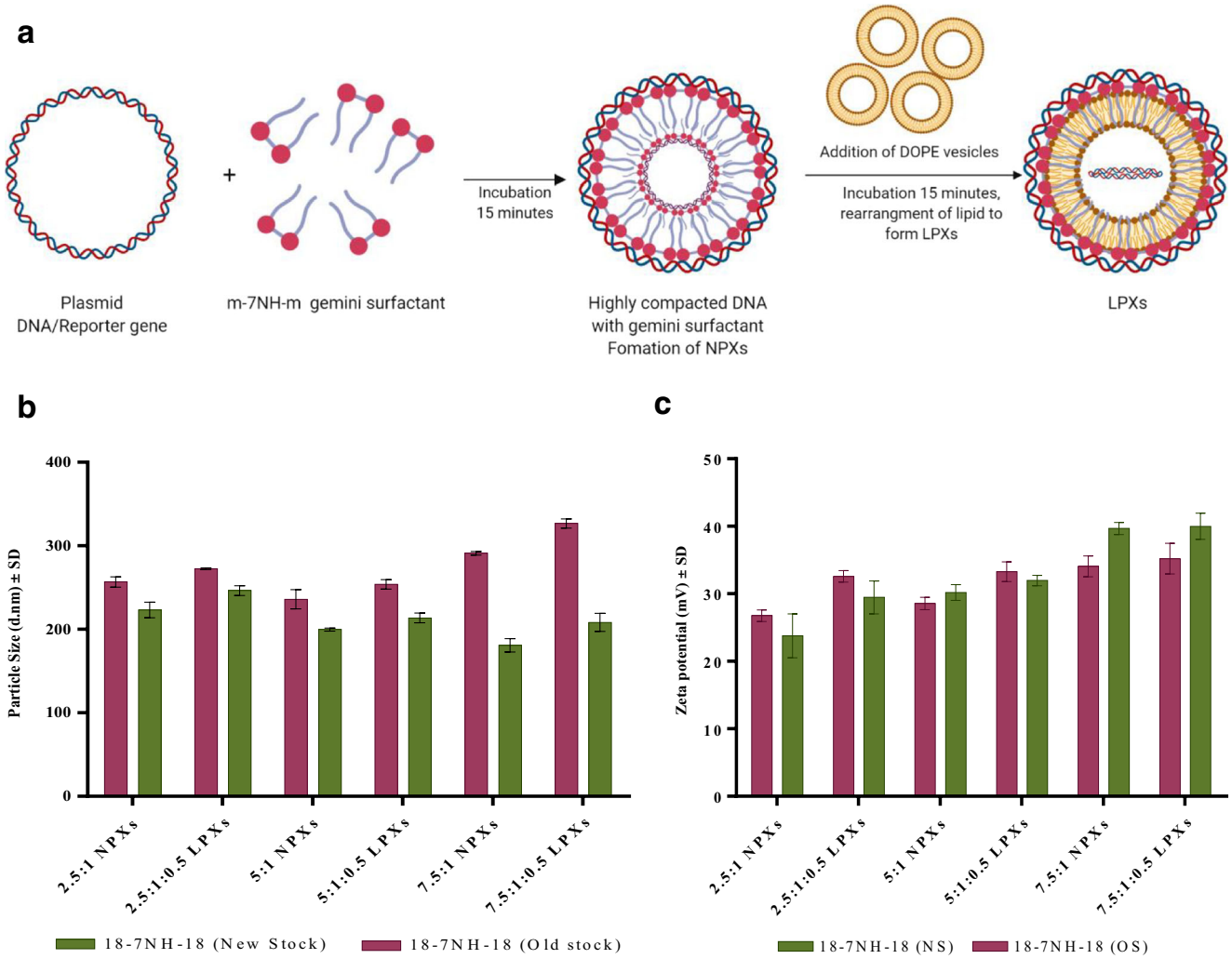

Fig. 2 Formulation and characterization of 18-7NH-18 NPXs made from material synthesized using new stock, (NS), (**a**) Schematic diagram of the formulation of gemini-plasmid NPXs and gemini-plasmid-lipid LPXs, (**b**) Particle size distribution of m-7NH-m (OS and NS) at varying charge ratios, (**c**) Effect of ρ ± on zeta potential of m-7NH-m (OS and NS) NPXs.

NPXs made with 18-7NH-18 gemini surfactant using both the old and the new improved method (labelled as old and new stocks (OS and NS)) showed some differences in particle size with respect to ρ±. The particle size of NPXs and LPXs made from the 18-7NH-18 new stock was generally lower at all three ρ ± (Fig. 2b). As the ρ ± increased, zeta potential of the 18-7NH-18 NPXs and LPXs, both NS and OS, also increased (Fig. 2c). The increase in zeta potential for LPXs was generally smaller compared to NPXs across the three different ratios, which was expected as DOPE is a neutral lipid, but adding DOPE correlated with an increase in particle size of 18-7NH-18 LPXs. The optimal TE was achieved with 18-7NH-18 NPXs at ρ ± 5:1 with a mean particle size of 199.8 ± 1.83 nm ± S.D. and zeta potential of +30.18 ± 1.17 mV ± S.D. (Fig. 2b and c, Fig. 3a).

NPXs made using 18-7NH-18 gemini surfactant OS and NS at ρ ± 2.5:1, 5:1, 7.5:1 and 10:1 showed that the TE of 18-7NH-18 OS-NPXs was significantly lower compared to the 18-7NH-18 NS-NPXs treatment at all ratios, 1.21 ± 0.1%, 2.79 ± 0.3%, 3.020 ± 0.76% and 2.833 ± 0.51% for 18-7NH-18 OS-NPXs and 4.66 ± 0.4%, 10.97 ± 0.11%, 8.96 ± 0.16% and 8.33 ± 0.22% for 18-7NH-18 NS-NPXs, respectively ($p < 0.0001$) (Fig. 3a). The TE of the 18-7NH-18 NS-NPXs increased up to 5:1 ratio then decreased with increasing ρ ± (Fig. 3a). Statistical analysis confirmed that 18-7NH-18 NS-NPX treated cells consistently showed higher TE compared to 18-7NH-18 OS-NPX treatment at 48 h ($p < 0.0001$) (Fig. 3a). Generally, the viability of both 18-7NH-18 NS-NPX and 18-7NH-18 OS-NPX treated A7 astrocytes decreased with increasing ρ±, 75.37 ± 1.03%, 62.47 ± 2.02, 42.71 ± 2.606 and 46.63 ± 2.53 for 18-7NH-18 OS-NPXs and 95.55 ± 0.50%, 92.97 ± 0.57%, 90.18 ± 0.43% and 87.91 ± 1.17% for 18-7NH-18 NS-NPXs at 2.5:1, 5:1, 7.5:1 and 10:1 ratios, respectively (Fig. 3b). Overall, 18-7NH-18

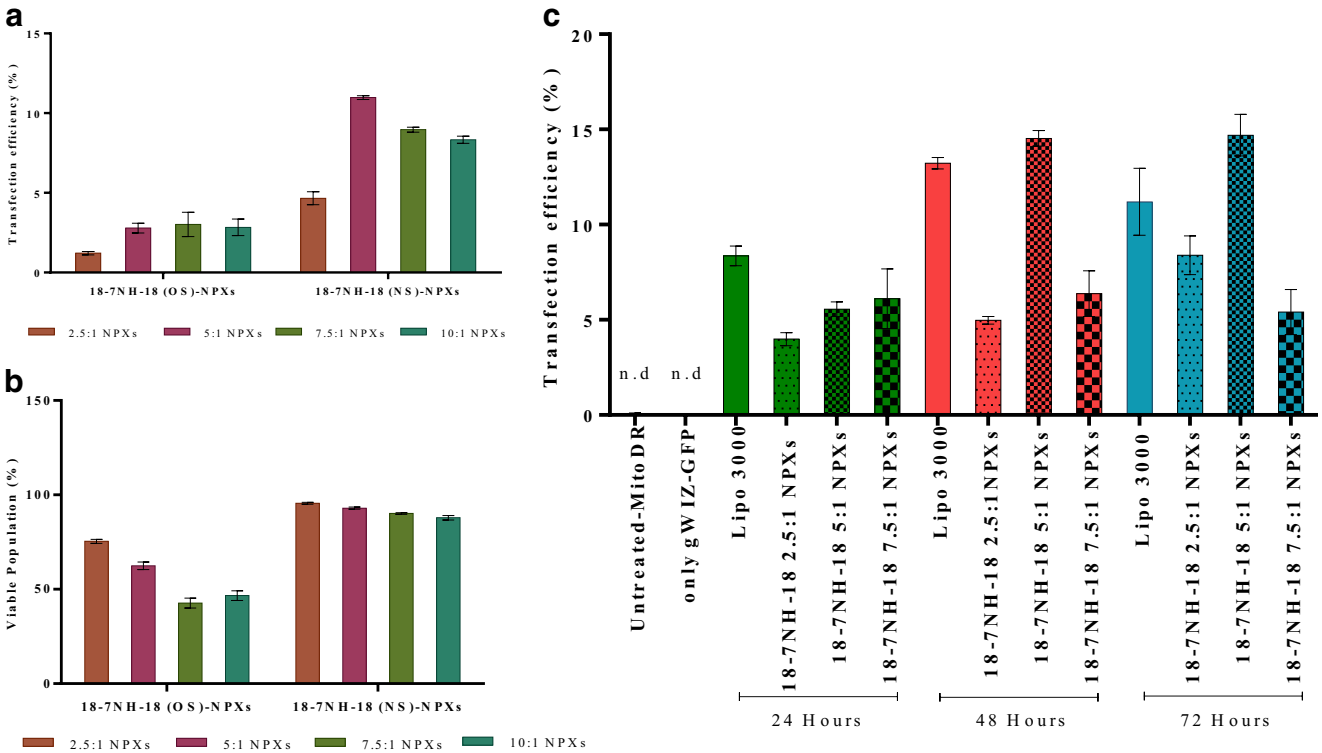

Fig. 3 Transfection efficiency and biocompatibility of 18-7NH-18 NPXs made from material synthesized using method 1 and method 2 (old method stock, (OS) and new method stock (NS), (**a**) Assessment of TE of 18-7NH-18 (OS) and 18-7NH-18 (NS) in A7 astrocytes by flow cytometry using gWIZ plasmid encoding GFP as a reporter gene. TE of 18-7NH-18 (NS) NPX treatments are significantly higher ($p < 0.0001$) compared to 18-7NH-18 (OS) NPXs at all ratios tested, 18-7NH-18 (NS) 5:1 NPXs have shown significantly higher TE compared with 2.5:1, 10:1 ($p < 0.0001$) and 7.5:1 ($p < 0.001$). All values expressed as mean ± S.D. ($n = 3$), (**b**) Viability profile of A7 astrocytes treated with 18-7NH-18 NPXs (OS and NS).=, Viability was assessed by flow cytometry using MitoTracker® Deep Red. Viability of 18-7NH-18 (NS) NPX treatments are significantly higher ($p < 0.0001$) compared to 18-7NH-18 (OS) NPXs at all ratios tested. Values expressed as mean ± S.D. (n = 3), (**c**) Gene expression kinetics studies. TE in A7 cells treated with 18-7NH-18 NPXs, treatments were removed at 5 h and evaluated at 24, 48 and 72 h. TE was measured by flow cytometry tracking GFP expression. TE of 18-7NH-18 (NS) 5:1 NPX treatments at 48 and 72 h are significantly higher ($p < 0.0001$) compared to 18-7NH-18 (NS) 5:1 NPXs at 24 h. No significant difference in the TE was observed between 48 and 72 h for 18-7NH-18 (NS) 5:1 NPXs treatment. All values expressed as mean ± S.D.(n = 3), (n.d. - not detected).

NS-NPXs treated cells had significantly higher viabilities compared to 18-7NH-18 OS-NPXs treated cells ($p < 0.0001$), which could be attributed to the presence of trimeric m-7 N(m)-m gemini surfactant and DMAP impurities.

As part of the optimization with respect to *in vitro* gene expression kinetics and the use of DOPE as a nanoparticle component several experiments were performed. Assessment of the kinetics of gene expression over time demonstrated that TE was the highest at 48 h after treatment application with the m-7NH-m NPXs (Fig. 3c). At the 48-h time point the 18-7NH-18 5:1 NPXs had the highest TE of $14.53 \pm 0.41\%$ compared to $5.55 \pm 0.38\%$ at 24 h ($p < 0.0001$) with no further increase at 72 h ($14.69 \pm 1.094\%$).

To assess the effect of DOPE on TE and viability of cells, we formulated two sets of LPX formulations with the same ρ±, such as 2.5:1, 5:1, 7.5:1, 10:1 and 12.5:1 (G:P) and with (1:0.5, 1:1, 1:1.5 and 1:2 G:L ratios), as well as without DOPE. The flow cytometry results demonstrated that increasing DOPE in the formulation resulted in a decrease of TE. The 1:0.5 ratio of DOPE had significantly higher TE compared to higher ratios ($p < 0.0001$) (Fig. 4a), therefore in all other studies the 1:0.5 G:L ratio was used for LPX formulations. Transfection with Lipofectamine 3000 showed similar kinetics to NPXs as TE increased over time (higher TE at 48 h compared to 24 h;$13.22 \pm 0.30\%$ *vs.* $8.35 \pm 0.51\%$) (Fig. 2c), but the peak gene expression was higher with gemini NPXs at 48 h ($14.53 \pm 0.41\%$).

Results from the confocal microscopic imaging studies were in agreement with the flow cytometry results and confirmed that TE was highest with 18-7NH-18 5:1 NPXs compared to other ρ ± tested. Whereas cells treated with LPXs with ρ ± 5:1 and G:L ratio of 1:0.5 had lower TE and higher cell toxicities compared to 18-7NH-18 5:1 NPXs (without DOPE) at 48 h (Fig. 4b). The results demonstrate that DOPE inclusion in the formulations, even at lower concentrations, caused cytotoxicity. At 72 h there was still a low level of GFP and Mitrotracker red fluorescence was observed in the NPX treated wells, there was no GFP or Mitotracker red fluorescence observed due the greatly reduced cell numbers after treatment with DOPE containing LPXs.

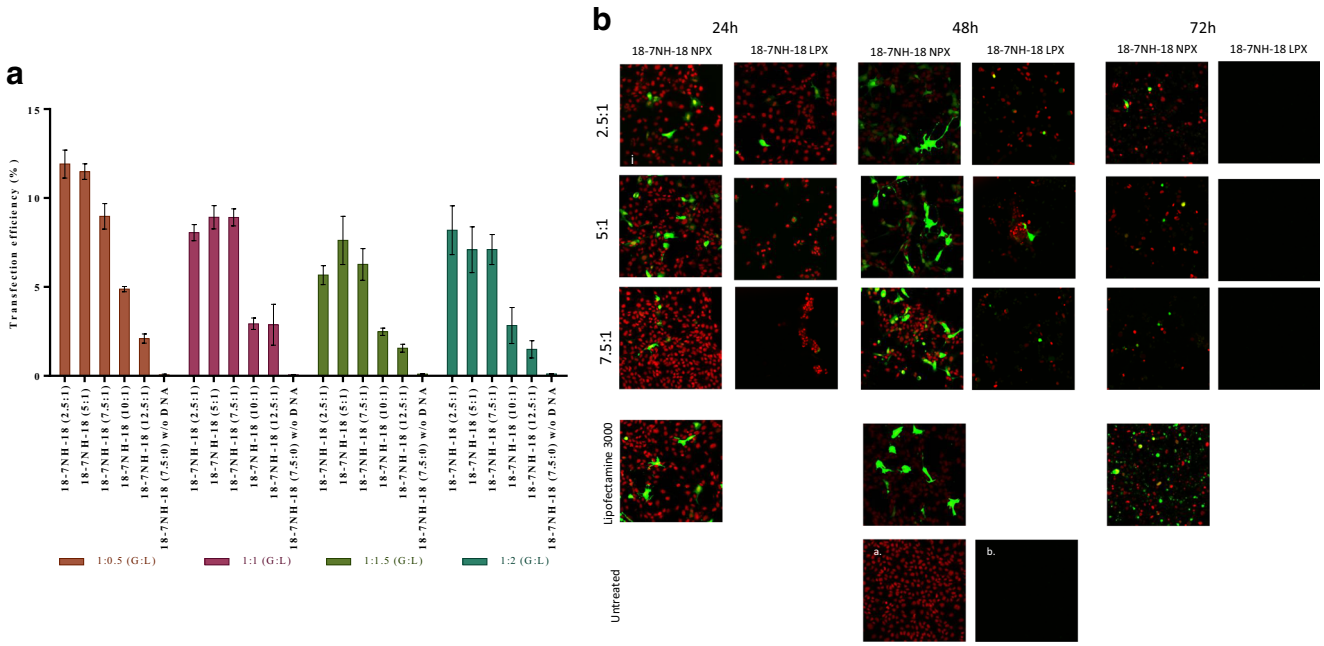

Fig. 4 Flow cytometry and confocal microscopy studies of the effect of DOPE on TE and toxicity of LPXs in A7 astrocytes, (**a**) Effect of G:L ratio on TE of 18-7NH-18 NPXs prepared with 2.5:1, 5:1, 7.5:1, 10:1 and 12.5:1 ρ ± ratios. At each ρ ± ratio DOPE was added at 1:0.5, 1:1, 1:1.5, and 1:3 G:L mass ratio. TE using18-7NH-18 2.5:1 and 5:1 (G:P) NPXs at 1:0.5 (G:L) ratio is significantly higher ($p < 0.0001$) compared to 1:1,1:1.5 and 1:2; no significant difference (n.s) in TE was observed between 1:1.5 and 1:2 G:L mass ratio, (**b**) Confocal microscopic images of A7 astrocytes treated with NPXs and LPXs. TE (green GFP expression) is shown at 24, 48 and 72 h for 18-7NH-18 NPXs prepared with 2.5:1, 5:1 and 7.5:1 ρ ± ratios and respective LPXs with DOPE at 1:0.5 G:L mass ratio. MitoTracker Deep Red was used as cell viability stain. Lipofectamine 3000 was used as a reference transfection agent and untreated cells as control. (**a**) treated with Mitotracker Deep Red (**b**) untreated and unstained.

DOPE, a neutral helper lipid, is frequently used in nanoparticles to facilitate gene delivery due to its ability to form inverted hexagonal (H_{II}) polymorphic structures with membrane fusogenic functions. DOPE may facilitate cellular uptake or endosomal escape by membrane fusion (27,28). Recent reports indicate that DOPE can also contribute to cell toxicity and notably it is known to perform better *in vitro* but often fails *in vivo* (29,30). In the current study it was also confirmed that DOPE at low levels (1: 0.5 ratio) was useful to enhance TE without lowering cell viability, however, 18-7NH-18 NPX formulations without DOPE lipid comparatively performed better than 18-7NH-18 LPXs. The 18-7NH-18 2.5:1:0.5 LPXs (G:P:L) produced similar TE as 18-7NH-18 5:1 NPXs without DOPE. This effect could be due to similar levels of fusogenic or temporary membrane disruption effects with the 18-7NH-18 2.5:1:0.5 LPXs and 18-7NH-18 5:1 NPXs.

With the addition of DOPE at increasing ratios, the increase in lipid concentration lowers ρ ± and charge density that may also decrease TE (31). In addition, the overall concentration of both gemini surfactant and DOPE in the nanoparticles is also important to achieve optimum function and biocompatibility (32,33), therefore tuning of composition for each specific gemini surfactant nanoparticle system is necessary. In a recent paper, we showed by theoretical modeling studies combined with experimental data that the DOPE concentration and charge ratio have specific importance. It was shown that the NPs at DOPE: gemini ratio 2–3 and gemini surfactant cationic charge ratio of 2.7, at pH 5 form a stable fusogenic lamellar/H_{II} structure, characterized by a low free energy value, which play a role in endosomal escape leading to higher TE (34).

The development of nanoparticles as a non-invasive topical eye drop dosage form requires information about penetration or crossing the corneal tissue. We used the 3D human EpiCorneal™ tissue model by MatTek, which is a human corneal epithelial cell culture at an air/liquid interface forming multilayered corneal tissue equivalent. The tissue typically contains 4–5 epithelial cell layers on a support membrane with cellular features such as desmosomes, tight junctions and microvilli and functionalities to express cytokines and disease markers and permeability properties similar to human cornea. Generally, the thickness of the corneal tissue model varied between 60 and 120 μm, based on confocal microscopic z-stack scanning of the 24 tissues in the plate. The NPXs strongly interacted with the corneal tissue even after three repetitive steps of washing (to simulate removal of surface-bound NPXs by tear) before imaging. The 18-7NH-18 5:1 NPXs carrying Cy5 labelled gWIZ-GFP plasmid penetrated approximately 80-100 μm deep into the corneal tissue within the first 0.5–1 h (Fig. 5a).

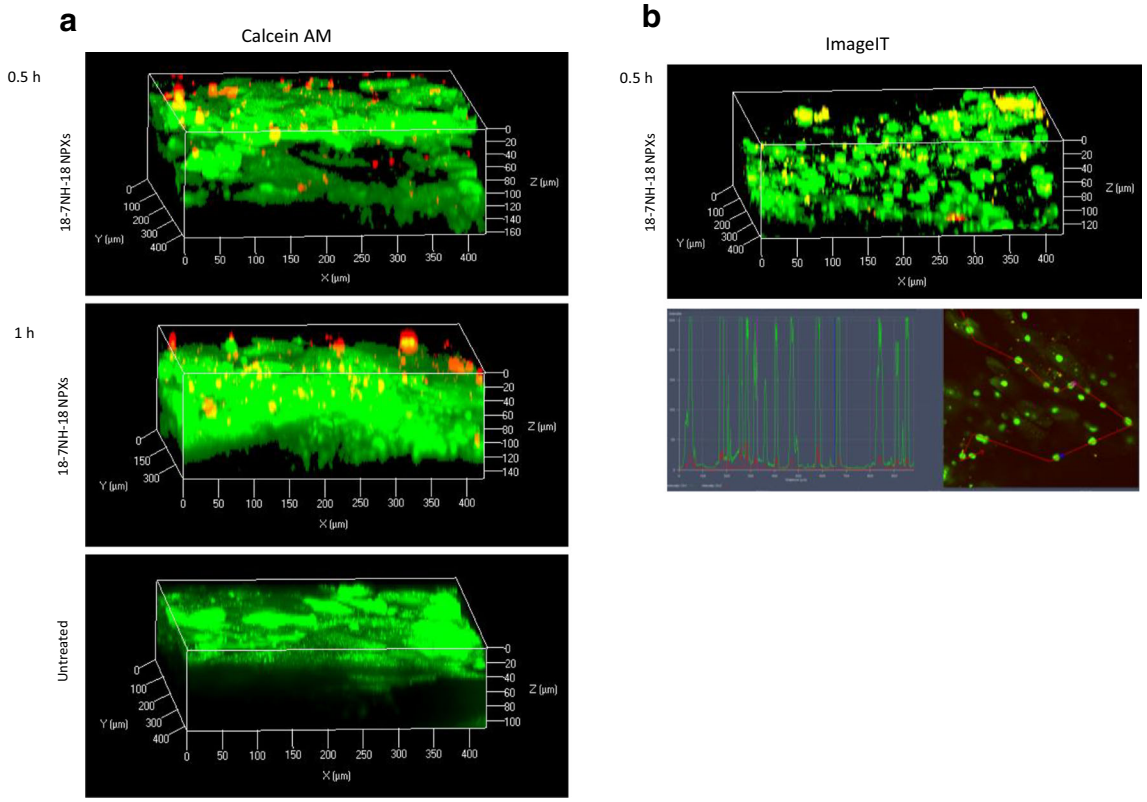

Fig. 5 Evaluation of *in vitro* corneal penetration of 18-7NH-18 NPXs. Confocal microscopic images of 3D EpiCorneal tissues treated with 18-7NH-18 NPXs carrying Cy5-labelled plasmid for 0.5 and 1 h. (**a**) z-stack images of corneas counter stained with Calcein AM viability stain (green) along with untreated cornea with Calcein AM viability stain; and (**b**) z-stack of the cornea treated for 0.5 h with 18-7NH-18 NPXs and stained with Image IT dead cell stain (green) and corresponding profile and fluorescence intensity graph showing colocalization of cells (green) with NPXs (red).

This is indicative of the possibility that given long enough residence time in the precorneal area, the nanoparticles may be able to cross the cornea and penetrate toward the posterior of the eye.

The NPXs penetrated into the tissue through the intercellular spaces to reach deeper layers of the corneal tissue. The 18-7NH-18 NPXs were also observed to be taken up into cells with in the first hour (Fig. 5a). It was observed that the intracellular NPXs were present in cells that counterstain with both Calcein AM and Image IT stain (Fig. 5b). This indicates that the uptake mechanism is related to the temporary permeabilization of the cellular membranes, hence allowing the Image IT stain (dead cell indicator, impermeant dye to healthy cells) to permeate into the cells, but at the same time the cells also stain positive with Calcein AM viability stain. We have shown before that gemini nanoparticles have the ability to interact with membranes and induce temporary increase of permeability by 'nanoporation' (35). This phenomenon is associated with the permeation of typically membrane-impermeable stains used for imaging studies (eg. dead-cell stains) but at the same time the cells also stain positive with metabolic cell viability dyes (eg. Mitotracker Deep Red or Calcein AM). In this confocal microscopic study, the Image IT dead cell stain stained the corneas treated with NPXs, but interestingly, the staining pattern corresponded to the pattern of NPX diffusion indicating that temporary cell membrane disruption was caused by the NPXs. However, the tissue appeared normalized several hours later and as the nanoparticles diffused out of the cornea, the membrane integrity recovered and the cells stained positive with Mitotracker Green at 24 h (results not shown).

CONCLUSIONS

We have formulated a novel gene delivery nanoparticle system based on the 18-7NH-18 s-generation gemini surfactant for gene therapy by ocular topical application. The m-7NH-m series of gemini surfactant building blocks were synthesized by an improved one-pot, DMAP free reaction scheme with 2-fold increase in yield and high purity without contamination of a previously unidentified trimeric gemini surfactant by-product (m-7N(m)-m) and DMAP.

NPXs made from 18-7NH-18 gemini surfactant made with the new synthetic scheme showed high TE and reduced

toxicities in A7 astrocytes at the optimum ρ ± 5:1 ratio. The presence of DOPE was shown to be detrimental for both transfection and cell viability, that is 18-7NH-18-NPXs consistently showed higher TE and cell viability compared to LPXs. *In vitro* corneal interaction assessment of the 18-7NH-18 NPXs showed penetration and crossing of the cornea within 0.5–1 h after treatment with low toxicity.

Overall, the NPXs made from 18-7NH-18 gemini surfactant are potential gene delivery systems for topical ophthalmic administration and for further *in vivo* studies.

Acknowledgments and Disclosures. The research in this paper was supported by operating and equipment grants from the Canadian Institutes of Health Research, the Natural Sciences and Engineering Research Council of Canada, the Canada Foundation for Innovation and the Ontario Research Fund. The generous support of the Canada Foundation for Innovation, the Ontario Research Fund and the Canada Research Chairs Program is also gratefully acknowledged (M. Foldvari).

REFERENCES

1. Bunton CA, Robinson LB, Schaak J, Stam M. Catalysis of nucleophilic substitutions by micelles of dicationic detergents. The Journal of Organic Chemistry. 1971;36(16):2346–50.
2. Deinega Y, Ulberg Z, Marochko L, Rudi V, Denisenko V. Investigation of colloid-chemical properties of surfactants of type of quaternary ammonium-compounds. Colloid J USSR. 1974;36(4):601–4.
3. Karaborni S, Esselink K, Hilbers P, Smit B, Karthauser J, Van Os N, et al. Simulating the self-assembly of gemini (dimeric) surfactants. Science. 1994;266(5183):254–6.
4. Menger FM, Keiper JS. Gemini surfactants. Angew Chem Int Ed. 2000;39(11):1906–20.
5. Kirby AJ, Camilleri P, Engberts JB, Feiters MC, Nolte RJ, Söderman O, et al. Gemini surfactants: new synthetic vectors for gene transfection. Angew Chem Int Ed. 2003;42(13):1448–57.
6. Badea I, Verrall R, Baca-Estrada M, Tikoo S, Rosenberg A, Kumar P, et al. In vivo cutaneous interferon-γ gene delivery using novel dicationic (gemini) surfactant-plasmid complexes. The journal of gene medicine. 2005;7(9):1200–14.
7. Wang C, Li X, Wettig SD, Badea I, Foldvari M, Verrall RE. Investigation of complexes formed by interaction of cationic gemini surfactants with deoxyribonucleic acid. Phys Chem Chem Phys. 2007;9(13):1616–28.
8. Wettig SD, Verrall RE, Foldvari M. Gemini surfactants: a new family of building blocks for non-viral gene delivery systems. Current gene therapy. 2008;8(1):9–23.
9. Ahmed T, Kamel AO, Wettig SD. Interactions between DNA and Gemini surfactant: impact on gene therapy: part I. Nanomedicine. 2016;11(3):289–306.
10. Muñoz-Úbeda M, Misra SK, Barrán-Berdón AL, Datta S, Aicart-Ramos C, Castro-Hartmann P, et al. How does the spacer length of cationic Gemini lipids influence the Lipoplex formation with plasmid DNA? Physicochemical and biochemical characterizations and their relevance in gene therapy. Biomacromolecules. 2012;13(12):3926–37.
11. Wettig S. D., Badea I, Donkuru M, Verrall RE, Foldvari M. structural and transfection properties of amine-substituted gemini surfactant-based nanoparticles. J Gene Med. 2007;9(8):649–58.
12. Wettig SD, Wang C, Verrall RE, Foldvari M. Thermodynamic and aggregation properties of aza- and imino-substituted gemini surfactants designed for gene delivery. Phys Chem Chem Phys. 2007;9(7):871–7.
13. Donkuru M, Wettig SD, Verrall RE, Badea I, Foldvari M. Designing pH-sensitive gemini nanoparticles for non-viral gene delivery into keratinocytes. J Mater Chem. 2012;22(13):6232–44.
14. Al-Dulaymi M, Michel D, Chitanda JM, El-Aneed A, Verrall RE, Grochulski P, et al. Molecular engineering as an approach to modulate gene delivery efficiency of peptide-modified Gemini surfactants. Bioconjug Chem. 2018;29(10):3293–308.
15. Mohammed-Saeid W, Chitanda J, Al-Dulaymi M, Verrall R, Badea I. Design and evaluation of RGD-modified Gemini surfactant-based Lipoplexes for targeted gene therapy in melanoma model. Pharm Res. 2017;34(9):1886–96.
16. Singh J, Yang P, Michel D, Verrall RE, Foldvari M, Badea I. Amino acid-substituted gemini surfactant-based nanoparticles as safe and versatile gene delivery agents. Current drug delivery. 2011;8(3):299–306.
17. Yang P, Singh J, Wettig S, Foldvari M, Verrall RE, Badea I. Enhanced gene expression in epithelial cells transfected with amino acid-substituted gemini nanoparticles. European journal of pharmaceutics and biopharmaceutics : official journal of Arbeitsgemeinschaft fur Pharmazeutische Verfahrenstechnik eV. 2010;75(3):311–20.
18. Menger FM, Littau CA. Gemini-surfactants: synthesis and properties. J Am Chem Soc. 1991;113(4):1451–2.
19. Menger FM, Littau CA. Gemini surfactants: a new class of self-assembling molecules. J Am Chem Soc. 1993;115(22):10083–90.
20. Zana R, Benrraou M, Rueff R. Alkanediyl-a, w-bis (dimethyl-alkyl ammonium bromide) surfactants. 1. Effect of the spacer chain length on the CMC and micelle ionization degree. Langmuir : the ACS journal of surfaces and colloids. 1991;7:1072–5.
21. Wettig SD, Verrall RE. Thermodynamic studies of aqueous m–s–m Gemini surfactant systems. J Colloid Interface Sci. 2001;235(2):310–6.
22. Elsabahy M, Badea I, Verrall R, Donkuru M, Foldvari M. Dicationic gemini nanoparticle design for gene therapy. In: John Wiley & Sons, Inc; 2013. p. 509–528.
23. Hayashi Y. Pot economy and one-pot synthesis. Chem Sci. 2016;7(2):866–80.
24. Raju M, Mäeorg S, Tšubrik O, Mäeorg U. Efficient solventless technique for Boc-protection of hydrazines and amines. Arkivoc. 2009;6:291–7.
25. Han Y, Wang Y. Aggregation behavior of gemini surfactants and their interaction with macromolecules in aqueous solution. Phys Chem Chem Phys. 2011;13(6):1939–56.
26. Zana R. Dimeric (Gemini) surfactants: effect of the spacer group on the association behavior in aqueous solution. J Colloid Interface Sci. 2002;248(2):203–20.
27. Liu F, Huang L. Development of non-viral vectors for systemic gene delivery. J Control Release. 2002;78(1):259–66.
28. Buck J, Grossen P, Cullis PR, Huwyler J, Witzigmann D. Lipid-based DNA therapeutics: hallmarks of non-viral gene delivery. ACS Nano. 2019;13(4):3754–82.
29. Song YK, Liu F, Chu S, Liu D. Characterization of cationic liposome-mediated gene *transfer* in vivo by intravenous administration. Hum Gene Ther. 1997;8(13):1585–94.
30. Audouy S, Molema G, de Leij L, Hoekstra D. Serum as a modulator of lipoplex-mediated gene transfection: dependence of amphiphile, cell type and complex stability. The Journal of Gene

Medicine: A cross-disciplinary journal for research on the science of gene transfer and its clinical applications. 2000;2(6):465–76.
31. Al-Dosari MS, Gao X. Nonviral gene delivery: principle, limitations, and recent Progress. AAPS J. 2009;11(4):671.
32. Beddoes CM, Case CP, Briscoe WH. Understanding nanoparticle cellular entry: a physicochemical perspective. Adv Colloid Interf Sci. 2015;218:48–68.
33. Munro S. Lipid rafts: elusive or illusive? Cell. 2003;115(4):377–88.
34. Taheri-Araghi S, Chen D-W, Kohandel M, Sivaloganathan S, Foldvari M. Tuning optimum transfection of gemini surfactant–phospholipid–DNA nanoparticles by validated theoretical modeling. Nanoscale. 2019;11(3):1037–46.
35. Gharagozloo M, Rafiee A, Chen DW, Foldvari M. A flow cytometric approach to study the mechanism of gene delivery to cells by gemini-lipid nanoparticles: an implication for cell membrane nanoporation. Journal of Nanobiotechnology. 2015;13(1):62.